2024 European Control Conference (ECC)
June 25-28, 2024. Stockholm, Sweden

Robust Nonlinear $\mathcal{W}_\infty$ Optimal Control for Input Nonaffine Systems*

Daniel N. Cardoso[1], Marco H. Terra[2] and Guilherme V. Raffo[1,3]

***Abstract*— We propose a novel robust nonlinear $\mathcal{W}_\infty$ optimal control method for dynamical systems with nonaffine control inputs. The nonlinear $\mathcal{W}_\infty$ control formulation extends the classic nonlinear $\mathcal{H}_\infty$ one, considering a weighted Sobolev norm of the cost variable. This approach assumes that the cost variable belongs to the weighted Sobolev space $\mathcal{W}_{m,p,\Gamma}$, ensuring continuity and differentiability up to degree m in a certain domain Ω. Consequently, in addition to the well-known features provided by the $\mathcal{H}_\infty$ approach in terms of disturbance attenuation, the closed-loop system benefits from the enhanced transient performance. Here, the robust nonlinear $\mathcal{W}_\infty$ optimal control problem is formulated via dynamic programming for increased-order systems, and a particular solution is proposed to the resulting Hamilton-Jacobi equation, along with the corresponding stability analysis. To validate the proposed method and its versatility, we provide numerical results for the control of a quadrotor. Additionally, leveraging the inherent $\mathcal{L}_2$-gain properties of our approach, we demonstrate that the resulting controller can achieve trajectory tracking with guaranteed asymptotic stability for the whole closed-loop system.**

I. INTRODUCTION

Input nonaffine systems are present in numerous real-world applications, encompassing fields such as aerospace [1], robotics [2], and chemical process [3]. This kind of systems exhibits nonlinearities with respect to the control input, hindering the use of classic linear and nonlinear control techniques in their control design. When designing controllers for input nonaffine systems, a common approach is to approximate the nonlinear function of the control input by an affine virtual control signal, assuming the availability of the direct inversion of the corresponding nonlinear function [1]. Although the existence of an inverse function can be guaranteed by the Implicit Function Theorem [4], this approach cannot be applied to all systems, as the inverse function might be difficult to obtain. Another approach is the control design based on the linearized model around an operating point. Nevertheless, the effectiveness of the resulting controller is ensured locally.

*This work was in part supported by the project INCT (National Institute of Science and Technology) for Cooperative Autonomous Systems Applied to Security and Environment under the grants CNPq 465755/2014-3 and FAPESP 2014/50851-0. This work was also supported in part by the Brazilian agencies Coordination for the Improvement of Higher Education Personnel - Brazil (CAPES) through the Academic Excellence Program (PROEX), CNPq under grants 317058/2023-1 and 422143/2023-5, and FAPEMIG under the grants APQ-03090-17 and BPD-00960-22.

[1]D. N. Cardoso and G. V. Raffo are with the Graduate Program in Electrical Engineering, Federal University of Minas Gerais, Belo Horizonte, MG, Brazil. {danielneri, raffo}@ufmg.br

[2]Marco. H. Terra is with the Department of Electrical and Computer Engineering, University of São Paulo, São Carlos, SP, Brazil. terra@sc.usp.br

[3]G.V. Raffo is with the Department of Electronics Engineering, Federal University of Minas Gerais (UFMG), Belo Horizonte, MG, Brazil.

Some approaches employ learning-based control methods, as in [5], to learn a corresponding adaptive closed-loop control law from the dynamics of nonaffine nonlinear systems. Conversely, in [6], the authors have proposed a systematic procedure in which the system is differentiated to obtain an increased-order system affine in the time derivative of the control signal. Control designs utilizing high-order derivatives have already been employed in the literature for mechanical systems [7], [8], [9]. In this context, the third time derivative of an object's position is referred to as jerk, while the fourth derivative is known as snap. Minimizing jerk and snap is often interesting because it allows a smooth and precise motion, ensuring the avoidance of abrupt changes.

In addition to the inherent challenges of designing controllers for input nonaffine systems, dynamical systems are frequently affected by disturbances from various sources, highlighting the need for robust controllers to guarantee stability and satisfactory performance. A usual approach to ensure these features is the well-known $\mathcal{H}_\infty$ control theory [10], which is formulated in the $\mathcal{L}_2$ space for nonlinear systems [11]. The $\mathcal{H}_\infty$ controller aims at minimizing the maximum gain given by the closed-loop system to a disturbance signal [12]. This type of controller has been applied to a wide variety of systems [13], [14], [15]. Besides the advantages, this control technique may present drawbacks. As stated in [16], the $\mathcal{H}_\infty$ control strategy deals mainly with the aspects of stabilization and disturbance attenuation and provides little control over the transient behavior.

An alternative approach involves formulating the $\mathcal{H}_\infty$ controller in Sobolev spaces $\mathcal{W}_{m,p}$. These spaces comprises functions in the $\mathcal{L}_p$ space whose generalized derivatives up to order m also belong to the $\mathcal{L}_p$ space [17]. This approach has been introduced in [18], where the $\mathcal{W}_{1,2}$-norm of the cost variable has been employed instead of the $\mathcal{L}_2$-norm. The resulting Optimal Control Problem (OCP) has been formulated using dynamic programming, requiring the solution of the related Hamilton-Jacobi (HJ) equation to obtain the corresponding controller. Solving Hamilton-Jacobi (HJ) Partial Differential Equations (PDEs) analytically for a general class of systems poses a considerable challenge. In particular, [18] has considered the HJ PDE resulting from the $\mathcal{H}_\infty$ control formulation in the Sobolev space to be intractable because of its complexity and has proposed an alternative approach through the backstepping technique to simplify the problem. However, the solution given by the backstepping approach has resulted quite similar to the classic nonlinear $\mathcal{H}_\infty$ one, differing by an integrator added to the cost variable. Hence, since the rate of change of the cost variable has not been accounted for in the cost functional, enhancements in the transient behavior have not been achieved.

Regarding the challenges in achieving solutions to HJ equations, it is common to employ numerical methods or seek specific solutions based on special classes of systems. In [19], an algorithm based on the Galerkin approximation has been proposed to obtain a solution to the HJ equation presented in [18]. Nevertheless, the solution is limited to a specific problem domain, in addition to the algorithm suffering from the curse of dimensionality, hindering its applicability to high-order systems. Conversely, in [20], the authors have formulated the nonlinear $\mathcal{H}_\infty$ controller in the $\mathcal{W}_{1,2}$ Sobolev space for the class of input affine fully actuated mechanical systems represented by the Euler-Lagrange equations. Due to the specific choice of the cost variable, the resulting HJ equation has become tractable, enabling the proposal of an analytical solution. Also, in [21], [22], the nonlinear $\mathcal{H}_\infty$ controller has been formulated in weighted Sobolev spaces to allow tuning component-wise the influences of the cost variable and its time derivatives in the control objectives. Particular solutions of the resulting HJ equations have been proposed for fully actuated, reduced underactuated, and underactuated with input coupling, input affine mechanical systems. A comparative analysis between the nonlinear $\mathcal{W}_\infty$[1] controller and the classic nonlinear $\mathcal{H}_\infty$ one has been presented, which has demonstrated that, besides robustness and simple design, the controller resulting from the weighted Sobolev approach has achieved better transient performance with a faster disturbance attenuation.

As the aforementioned controllers formulated in Sobolev spaces deal only with input affine nonlinear systems, in this work, with the goal of minimizing abrupt changes on the cost variable and being robust against exogenous disturbances, we extend such methodology to address the design of robust nonlinear $\mathcal{W}_\infty$ optimal controllers for nonautonomous dynamical systems with nonaffine control inputs. The main contributions of this paper are threefold: (i) a novel robust nonlinear $\mathcal{W}_\infty$ optimal control method to accommodate control input nonaffine dynamical systems with guaranteed asymptotic stability; (ii) the generalization of the proposed method for increased-order systems with any number of time derivatives; and (iii) the validation of the proposed control method when controlling a quadrotor. The latter is achieved by designing the proposed nonlinear $\mathcal{W}_\infty$ controller for both inner and outer loops of the interconnected dynamics of the quadrotor. Leveraging the inherent $\mathcal{L}_2$-gain properties of the proposed approach, trajectory tracking with asymptotic stability is guaranteed for the whole closed-loop system.

Notation: The notation used is standard. Italic lower case letters denote scalars, boldface italic lowercase letters denote vectors, and boldface italic uppercase letters denote matrices; $(\cdot)'$ and $(\cdot)^{-1}$ stand, respectively, for the transpose and inverse elements of $(\cdot)$; $\mathbb{N}\triangleq\{1,2,\ldots\}$, $\mathbb{R}\triangleq(-\infty,\infty)$, $\mathbb{R}_{\geq 0} \triangleq [0,\infty)$, $\mathbb{R}_{>0}\triangleq(0,\infty)$, $\mathbb{R}^n\triangleq\{\boldsymbol{r}=[r_1 \ \ldots \ r_n]':r_i\in\mathbb{R}\}$, and $\mathbb{R}^{n\times m}\triangleq\{\boldsymbol{R}=[\boldsymbol{r}_1 \ \ldots \ \boldsymbol{r}_m]:\boldsymbol{r}_i\in\mathbb{R}^n, i\in\{1,2,\cdots,m\}\}$; $\boldsymbol{0}$ and $\boldsymbol{I}$ are, respectively, zero and identity matrices with appropriate dimension; $\boldsymbol{z}(t):\mathbb{R}_{\geq 0}\to\mathbb{R}^{n_z}$ is a time-varying function, and $\dot{\boldsymbol{z}}(t)\triangleq d\boldsymbol{z}(t)/dt$, $\ddot{\boldsymbol{z}}(t)\triangleq d^2\boldsymbol{z}(t)/dt^2$, $\dddot{\boldsymbol{z}}(t)\triangleq d^3\boldsymbol{z}(t)/dt^3$, $\ddddot{\boldsymbol{z}}(t)\triangleq d^4\boldsymbol{z}(t)/dt^4$ and $\overset{(n)}{z}(t)\triangleq d^n\boldsymbol{z}(t)/dt^n$ denote the first, second, third, fourth and n-th time derivatives of $\boldsymbol{z}(t)$. If $\boldsymbol{z}(t)\in\mathcal{C}^p$, then $\overset{(1)}{\boldsymbol{z}}(t),\cdots,\overset{(p)}{\boldsymbol{z}}(t)$ exist and $\boldsymbol{z}(t)$ is continuous for any $t\in\mathbb{R}_{\geq 0}$. Let $t\in\mathbb{R}_{\geq 0}$, $p\in\mathbb{N}\cup\{\infty\}$, and $m\in\mathbb{N}\cup\{0\}$, therefore, $||\boldsymbol{z}(t)||_{\mathcal{L}_p,\boldsymbol{\Lambda}}\triangleq\left(\int_0^\infty ||\boldsymbol{\Lambda}^{1/p}\boldsymbol{z}(t)||_p^p \ dt\right)^{\frac{1}{p}}$, denotes the weighted $\mathcal{L}_p$-norm of $\boldsymbol{z}(t)$, where $\boldsymbol{\Lambda}$ is a symmetric and positive definite matrix. If $\boldsymbol{z}(t)\in\mathcal{L}_p[0,\infty)$, then $||\boldsymbol{z}(t)||_{\mathcal{L}_p}<\infty$. The Sobolev space $\mathcal{W}_{m,p}$ is the set of all functions $\boldsymbol{z}:\Psi\to\mathbb{R}^{n_z}$ defined on a domain Ψ to which the week derivatives of $\boldsymbol{z}$ up to degree m exist and belong to the $\mathcal{L}_p$ space. The weak derivatives of a function are the same as the classic derivatives when the latter exist. For functions defined in the time domain, $\Psi=\mathbb{R}_{\geq 0}$, the Sobolev norm of $z(t)$ is $||\boldsymbol{z}(t)||_{\mathcal{W}_{m,p}}\triangleq(\sum_{\alpha=0}^{m}||d^\alpha\boldsymbol{z}(t)/dt^\alpha||_{\mathcal{L}_p}^p)^{1/p}$ and its weighted Sobolev norm is $||\boldsymbol{z}(t)||_{\mathcal{W}_{m,p,\boldsymbol{\Gamma}}}\triangleq(\sum_{\alpha=0}^{m}||d^\alpha\boldsymbol{z}(t)/dt^\alpha||_{\mathcal{L}_p,\boldsymbol{\Gamma}_\alpha}^p)^{1/p}$, with $\boldsymbol{\Gamma}\triangleq\{\boldsymbol{\Gamma}_0,\ldots,\boldsymbol{\Gamma}_m\}$. Accordingly, if $\boldsymbol{z}(t)\in\mathcal{W}_{m,p}$, then $||\boldsymbol{z}(t)||_{\mathcal{W}_{m,p}}<\infty$. Also, $\boldsymbol{z}(t)\in\mathcal{W}_{m,p,\boldsymbol{\Gamma}}$ implies $\boldsymbol{z}(t)\in\mathcal{W}_{m,p}$.

II. ROBUST NONLINEAR $\mathcal{W}_\infty$ CONTROL DESIGN FOR INPUT NONAFFINE SYSTEMS

In this section, we develop the robust nonlinear $\mathcal{W}_\infty$ optimal controller for control input nonaffine, nonautonomous dynamical systems. The goal is to achieve trajectory tracking with guaranteed asymptotic stability, while providing robustness against exogenous disturbances with fast transient performance.

Consider a generic second-order control input nonaffine, nonautonomous dynamical system described by

$$\ddot{\boldsymbol{q}} = \boldsymbol{f}(\boldsymbol{q},\dot{\boldsymbol{q}},\boldsymbol{u},t) + \boldsymbol{w}(t), \tag{1}$$

where $t\in\mathbb{R}_{\geq 0}$ is the time variable, $\boldsymbol{q}(t):\mathbb{R}_{\geq 0}\to\mathbb{R}^{n_q}$, $\boldsymbol{u}(t):\mathbb{R}_{\geq 0}\to\mathbb{R}^{n_u}$ is the control input vector, and $\boldsymbol{w}(t):\mathbb{R}_{\geq 0}\to\mathbb{R}^{n_w}$ is the disturbance vector. It is assumed that $n_q = n_u = n_w$. To transform (1) into an input affine system, we take its time derivative[2]

$$\dddot{\boldsymbol{q}} = \frac{\partial\boldsymbol{f}}{\partial\boldsymbol{q}}\dot{\boldsymbol{q}} + \frac{\partial\boldsymbol{f}}{\partial\dot{\boldsymbol{q}}}\ddot{\boldsymbol{q}} + \frac{\partial\boldsymbol{f}}{\partial t} + \frac{\partial\boldsymbol{f}}{\partial\boldsymbol{u}}\dot{\boldsymbol{u}} + \dot{\boldsymbol{w}}. \tag{2}$$

Aiming to solve the trajectory tracking problem, we first define the tracking error vector as $\tilde{\boldsymbol{q}}(t)=\boldsymbol{q}(t)-\boldsymbol{q}_r(t)$, where $\boldsymbol{q}_r(t)\in\mathcal{C}^3$ is the desired reference. Accordingly, the tracking error dynamics is written as

$$\begin{aligned}\dddot{\tilde{\boldsymbol{q}}} &= \frac{\partial\boldsymbol{f}}{\partial\boldsymbol{q}}\dot{\boldsymbol{q}} + \frac{\partial\boldsymbol{f}}{\partial\dot{\boldsymbol{q}}}\ddot{\boldsymbol{q}} + \frac{\partial\boldsymbol{f}}{\partial t} + \frac{\partial\boldsymbol{f}}{\partial\boldsymbol{u}}\dot{\boldsymbol{u}} + \dot{\boldsymbol{w}} - \dddot{\boldsymbol{q}}_r,\\ &= \boldsymbol{h}(\boldsymbol{q},\dot{\boldsymbol{q}},\ddot{\boldsymbol{q}},\boldsymbol{u},t) + \boldsymbol{G}(\boldsymbol{q},\dot{\boldsymbol{q}},\boldsymbol{u},t)\dot{\boldsymbol{u}} + \dot{\boldsymbol{w}},\end{aligned} \tag{3}$$

with $\boldsymbol{h}(\boldsymbol{q},\dot{\boldsymbol{q}},\ddot{\boldsymbol{q}},\boldsymbol{u},t) \triangleq \frac{\partial\boldsymbol{f}}{\partial\boldsymbol{q}}\dot{\boldsymbol{q}} + \frac{\partial\boldsymbol{f}}{\partial\dot{\boldsymbol{q}}}\ddot{\boldsymbol{q}} + \frac{\partial\boldsymbol{f}}{\partial t} - \dddot{\boldsymbol{q}}_r$, and $\boldsymbol{G}(\boldsymbol{q},\dot{\boldsymbol{q}},\boldsymbol{u},t)\triangleq\partial\boldsymbol{f}/\partial\boldsymbol{u}$.

Assumption 1: Matrix $\boldsymbol{G}$ is invertible within Ω, i.e. rank$(\boldsymbol{G}) = n_q$, $\forall(\boldsymbol{q},\dot{\boldsymbol{q}},\boldsymbol{u},t)\in\Omega$, where Ω stands for the set of all configurations the system can assume.

Then, considering the state vector

$$\boldsymbol{x}(t) \triangleq \left[(\int_0^t\tilde{\boldsymbol{q}}(\tau)d\tau)' \quad \tilde{\boldsymbol{q}}' \quad \dot{\tilde{\boldsymbol{q}}}' \quad \ddot{\tilde{\boldsymbol{q}}}'\right]', \tag{4}$$

[1]The formulation of the nonlinear $\mathcal{H}_\infty$ controller in the weighted Sobolev space is here referred to as $\mathcal{W}_\infty$.

[2]For the sake of convenience, throughout the manuscript, some function dependencies are omitted.

the system can be represented in the state-space as follows

$$\dot{\boldsymbol{x}} = \overbrace{\begin{bmatrix} \mathbf{0} & \boldsymbol{I} & \mathbf{0} & \mathbf{0} \\ \mathbf{0} & \mathbf{0} & \boldsymbol{I} & \mathbf{0} \\ \mathbf{0} & \mathbf{0} & \mathbf{0} & \boldsymbol{I} \\ \mathbf{0} & \mathbf{0} & \mathbf{0} & \mathbf{0} \end{bmatrix} \boldsymbol{x} + \begin{bmatrix} \mathbf{0} \\ \mathbf{0} \\ \mathbf{0} \\ \boldsymbol{h} \end{bmatrix}}^{\bar{\boldsymbol{h}}} + \overbrace{\begin{bmatrix} \mathbf{0} \\ \mathbf{0} \\ \mathbf{0} \\ \boldsymbol{G} \end{bmatrix}}^{\bar{\boldsymbol{G}}} \dot{\boldsymbol{u}} + \overbrace{\begin{bmatrix} \mathbf{0} \\ \mathbf{0} \\ \mathbf{0} \\ \boldsymbol{I} \end{bmatrix}}^{\bar{\boldsymbol{K}}} \dot{\boldsymbol{w}},$$

which is placed in the following standard form:

$$\mathcal{P}: \begin{cases} \dot{\boldsymbol{x}}(t) = \bar{\boldsymbol{h}} + \bar{\boldsymbol{G}}\dot{\boldsymbol{u}}(t) + \bar{\boldsymbol{K}}\dot{\boldsymbol{w}}(t), \quad \boldsymbol{x}(0) = \boldsymbol{x}_0, \\ \boldsymbol{z}(t) = \int_0^t \tilde{\boldsymbol{q}}(\tau) d\tau, \end{cases} \tag{5}$$

where $\boldsymbol{z}(t)$ is the cost variable, selected as an integral action over the tracking error $\tilde{\boldsymbol{q}}$ to provide parametric uncertainty and constant disturbance rejection capability for the closed-loop system.

Assumption 2: The state vector $\boldsymbol{x}(t)$, given by (4), is available by measurement or estimation.

With the goal of achieving an upper bound to the energy of the cost variable $\boldsymbol{z}(t)$ and its time derivatives up to degree four, and the energy of the disturbance $\dot{\boldsymbol{w}}(t)$,

$$||\boldsymbol{z}(t)||_{\mathcal{W}_{4,2,\Gamma}} \leq \gamma ||\dot{\boldsymbol{w}}(t)||_{\mathcal{L}_2}, \tag{6}$$

for any $\dot{\boldsymbol{w}}(t) \in \mathcal{L}_2$, in which γ is the $\mathcal{W}_\infty$ attenuation level [21], the robust nonlinear $\mathcal{W}_\infty$ control problem is posed as

$$\min_{\dot{\boldsymbol{u}} \in \mathcal{U}} \max_{\dot{\boldsymbol{w}} \in \mathcal{L}_2} \mathcal{J}, \tag{7}$$

in which the cost functional, $\mathcal{J}$, is given by

$$\begin{aligned} \mathcal{J} &\triangleq \frac{1}{2} ||\boldsymbol{z}(t)||^2_{\mathcal{W}_{4,2,\Gamma}} - \frac{1}{2}\gamma^2 ||\dot{\boldsymbol{w}}(t)||^2_{\mathcal{L}_2}, \\ &= \frac{1}{2} \left(\sum_{\alpha=0}^{4} \left|\left| \frac{d^\alpha \boldsymbol{z}(t)}{dt^\alpha} \right|\right|^2_{\mathcal{L}_2, \boldsymbol{\Gamma}_\alpha} \right) - \frac{1}{2}\gamma^2 ||\dot{\boldsymbol{w}}(t)||^2_{\mathcal{L}_2}, \end{aligned} \tag{8}$$

where $\boldsymbol{\Gamma} = \{\boldsymbol{\Gamma}_0, \boldsymbol{\Gamma}_1, \boldsymbol{\Gamma}_2, \boldsymbol{\Gamma}_3, \boldsymbol{\Gamma}_4\}$, in which $\boldsymbol{\Gamma}_i$, for $i \in \{0, 1, 2, 3, 4\}$, is a tuning matrix.

Remark 1: The OCP (7) is formulated under the assumption that $\boldsymbol{z}(t)$ belongs to the weighted Sobolev space $\mathcal{W}_{4,2,\Gamma}$, ensuring the continuity and differentiability of $\boldsymbol{z}(t)$ up to its four-time derivative. Consequently, the tracking error dynamics (3) is directly considered into the cost functional (8). As shown in [21], this approach provides the closed-loop system with an anticipatory capability, enhancing transient performance and enabling faster disturbance attenuation compared to the nonlinear $\mathcal{H}_\infty$ controller.

Remark 2: In contrast to the nonlinear $\mathcal{H}_\infty$ optimal control approach, the OCP (7) does not necessitate $\boldsymbol{u}$ or $\dot{\boldsymbol{u}}$ to belong to the $\mathcal{L}_2$ space as these signals are not directly weighted into the cost functional. This feature enables the $\mathcal{W}_\infty$ OCP (7) to be well-posed for systems in which $\boldsymbol{u}(t) \neq 0$ and $\dot{\boldsymbol{u}} \neq 0$ in steady-state conditions.

The OCP (7) is formulated here via dynamic programming [23], using differential game theory. The HJBI (Hamilton-Jacobi-Bellman-Isaacs) equation associated with this problem is given by

$$\frac{\partial V_\infty}{\partial t} + \min_{\dot{\boldsymbol{u}} \in \mathcal{U}} \max_{\dot{\boldsymbol{w}} \in \mathcal{L}_2} \left\{ \mathcal{H}\left(\frac{\partial V}{\partial \boldsymbol{x}}, \boldsymbol{x}, \boldsymbol{u}, \dot{\boldsymbol{u}}, \dot{\boldsymbol{w}}, t \right) \right\} = 0, \tag{9}$$

with the Hamiltonian

$$\begin{aligned} \mathcal{H} = \frac{\partial V}{\partial \boldsymbol{x}} \dot{\boldsymbol{x}} + \frac{1}{2} \boldsymbol{x}' \begin{bmatrix} \boldsymbol{\Gamma}_0 & \mathbf{0} & \mathbf{0} & \mathbf{0} \\ \mathbf{0} & \boldsymbol{\Gamma}_1 & \mathbf{0} & \mathbf{0} \\ \mathbf{0} & \mathbf{0} & \boldsymbol{\Gamma}_2 & \mathbf{0} \\ \mathbf{0} & \mathbf{0} & \mathbf{0} & \boldsymbol{\Gamma}_3 \end{bmatrix} \boldsymbol{x} + \frac{1}{2} \dddot{\tilde{\boldsymbol{q}}}' \boldsymbol{\Gamma}_4 \dddot{\tilde{\boldsymbol{q}}} \\ - \frac{1}{2}\gamma^2 \dot{\boldsymbol{w}}' \dot{\boldsymbol{w}}, \end{aligned} \tag{10}$$

and boundary condition $V_\infty(\mathbf{0}, t) = 0$.

The optimal control law, $\dot{\boldsymbol{u}}^*$, and the worst case of the disturbances, $\dot{\boldsymbol{w}}^*$, are computed by taking the following partial derivatives of (10):

$$\frac{\partial \mathcal{H}}{\partial \dot{\boldsymbol{u}}} = \bar{\boldsymbol{G}}' \frac{\partial V}{\partial \boldsymbol{x}} + \boldsymbol{G}' \boldsymbol{\Gamma}_4 \boldsymbol{G} \dot{\boldsymbol{u}} + \boldsymbol{G}' \boldsymbol{\Gamma}_4 \boldsymbol{h} + \boldsymbol{G}' \boldsymbol{\Gamma}_4 \dot{\boldsymbol{w}} = \mathbf{0}, \tag{11}$$

$$\frac{\partial \mathcal{H}}{\partial \dot{\boldsymbol{w}}} = \bar{\boldsymbol{K}}' \frac{\partial V}{\partial \boldsymbol{x}} + \boldsymbol{\Gamma}_4 \dot{\boldsymbol{w}} + \boldsymbol{\Gamma}_4 \boldsymbol{h} + \boldsymbol{\Gamma}_4 \boldsymbol{G} \dot{\boldsymbol{u}} - \gamma^2 \dot{\boldsymbol{w}} = \mathbf{0}. \tag{12}$$

Manipulating (11), we obtain the optimal control law

$$\dot{\boldsymbol{u}}^* = -\left(\boldsymbol{G}' \boldsymbol{\Gamma}_4 \boldsymbol{G} \right)^{-1} \left(\bar{\boldsymbol{G}}' \frac{\partial V}{\partial \boldsymbol{x}} + \boldsymbol{G}' \boldsymbol{\Gamma}_4 \boldsymbol{h} + \boldsymbol{G}' \boldsymbol{\Gamma}_4 \dot{\boldsymbol{w}} \right). \tag{13}$$

In addition, premultiplying (11) by $(\boldsymbol{G}')^{-1}$ and subtracting (12) from the result, we obtain

$$\dot{\boldsymbol{w}}^* = -\frac{1}{\gamma^2} \left((\boldsymbol{G}')^{-1} \bar{\boldsymbol{G}}' - \bar{\boldsymbol{K}}' \right) \frac{\partial V}{\partial \boldsymbol{x}} = 0. \tag{14}$$

Through the second order partial derivatives of (10), $\partial^2 \mathcal{H} / \partial \dot{\boldsymbol{u}}^2 = \boldsymbol{G}' \boldsymbol{\Gamma}_4 \boldsymbol{G} > 0$ and $\partial^2 \mathcal{H} / \partial \dot{\boldsymbol{w}}^2 = \boldsymbol{\Gamma}_4 + \gamma^2 \boldsymbol{I} < \mathbf{0}$, it can be verified that (13) and (14) are Min-Max extremum of the optimization problem, where the $\mathcal{W}_\infty$ attenuation level, γ, must be selected such that the last inequality holds.

The HJ PDE associated with (7) is obtained by replacing the optimal control law (13) and the worst case of the disturbances (14) in (9), yielding

$$\frac{\partial V}{\partial t} + \mathcal{H}\left(\partial V / \partial \boldsymbol{x}, \boldsymbol{x}, \boldsymbol{u}, \dot{\boldsymbol{u}}^*, \dot{\boldsymbol{w}}^*, t \right) = 0. \tag{15}$$

In the following theorem, we propose a particular solution for the HJ equation (15).

Theorem 1: Let V be the parameterized scalar function

$$V(\boldsymbol{x}) = \boldsymbol{x}' \boldsymbol{P} \boldsymbol{x} > 0, \tag{16}$$

such that matrix $\boldsymbol{P} > 0$ is obtained by solving the Riccati equation

$$-\boldsymbol{P}\boldsymbol{B}\boldsymbol{P} + \boldsymbol{A}\boldsymbol{P} + \boldsymbol{P}\boldsymbol{A}' + \boldsymbol{Q} = \mathbf{0}, \tag{17}$$

with

$$\boldsymbol{A} \triangleq \begin{bmatrix} \mathbf{0} & \boldsymbol{I} & \mathbf{0} & \mathbf{0} \\ \mathbf{0} & \mathbf{0} & \boldsymbol{I} & \mathbf{0} \\ \mathbf{0} & \mathbf{0} & \mathbf{0} & \boldsymbol{I} \\ \mathbf{0} & \mathbf{0} & \mathbf{0} & \mathbf{0} \end{bmatrix}, \boldsymbol{B} \triangleq \begin{bmatrix} \mathbf{0} & \mathbf{0} & \mathbf{0} & \mathbf{0} \\ \mathbf{0} & \mathbf{0} & \mathbf{0} & \mathbf{0} \\ \mathbf{0} & \mathbf{0} & \mathbf{0} & \mathbf{0} \\ \mathbf{0} & \mathbf{0} & \mathbf{0} & \boldsymbol{\Gamma}_4^{-1} \end{bmatrix},$$

$$\boldsymbol{Q} \triangleq \text{blkdiag}(\boldsymbol{\Gamma}_0, \boldsymbol{\Gamma}_1, \boldsymbol{\Gamma}_2, \boldsymbol{\Gamma}_3).$$

Then, (16) is a solution to the HJ equation (15).

Proof: The proof is conducted by replacing (16) in (15). In the following, the computation is performed in parts. Consider the HJ equation (15), since (16) is a time-invariant function, we have that $\frac{\partial V}{\partial t} = \mathbf{0}$, and (15) results in

$$\mathcal{H}\left(\frac{\partial V}{\partial \boldsymbol{x}}, \boldsymbol{x}, \boldsymbol{u}, \dot{\boldsymbol{u}}^*, \dot{\boldsymbol{w}}^*, t \right) = 0, \tag{18}$$

$$\frac{\partial V}{\partial \boldsymbol{x}} \dot{\boldsymbol{x}} + \frac{1}{2} \boldsymbol{x}' \begin{bmatrix} \boldsymbol{\Gamma}_0 & \mathbf{0} & \mathbf{0} & \mathbf{0} \\ \mathbf{0} & \boldsymbol{\Gamma}_1 & \mathbf{0} & \mathbf{0} \\ \mathbf{0} & \mathbf{0} & \boldsymbol{\Gamma}_2 & \mathbf{0} \\ \mathbf{0} & \mathbf{0} & \mathbf{0} & \boldsymbol{\Gamma}_3 \end{bmatrix} \boldsymbol{x} + \frac{1}{2} \dddot{\tilde{\boldsymbol{q}}}' \boldsymbol{\Gamma}_4 \dddot{\tilde{\boldsymbol{q}}} = 0. \tag{19}$$

In addition, considering (14) and (16), the optimal control law (13) is given by

$$\dot{\boldsymbol{u}}^* = -\left(\boldsymbol{G}' \boldsymbol{\Gamma}_4 \boldsymbol{G} \right)^{-1} \left(\bar{\boldsymbol{G}}' \boldsymbol{P} \boldsymbol{x} + \boldsymbol{G}' \boldsymbol{\Gamma}_4 \boldsymbol{h} \right), \tag{20}$$

which leads to the following closed-loop dynamics:

$$\dddot{\tilde{q}} = \begin{bmatrix} \mathbf{0} & \mathbf{0} & \mathbf{0} & \mathbf{\Gamma}_4^{-1} \end{bmatrix} \boldsymbol{P}\boldsymbol{x}, \tag{21}$$

which in the state-space is given by

$$\dot{\boldsymbol{x}} = \begin{bmatrix} \mathbf{0} & \boldsymbol{I} & \mathbf{0} & \mathbf{0} \\ \mathbf{0} & \mathbf{0} & \boldsymbol{I} & \mathbf{0} \\ \mathbf{0} & \mathbf{0} & \mathbf{0} & \boldsymbol{I} \\ \mathbf{0} & \mathbf{0} & \mathbf{0} & \mathbf{0} \end{bmatrix} \boldsymbol{x} - \begin{bmatrix} \mathbf{0} & \mathbf{0} & \mathbf{0} & \mathbf{0} \\ \mathbf{0} & \mathbf{0} & \mathbf{0} & \mathbf{0} \\ \mathbf{0} & \mathbf{0} & \mathbf{0} & \mathbf{0} \\ \mathbf{0} & \mathbf{0} & \mathbf{0} & \mathbf{\Gamma}_4^{-1} \end{bmatrix} \boldsymbol{P}\boldsymbol{x}. \tag{22}$$

Then, replacing (21) and (22) in the HJ equation (18), and decomposing the resulting equation in its symmetric and skew-symmetric components, it yields

$$\boldsymbol{x}' \left(-\boldsymbol{PBP} + \boldsymbol{AP} + \boldsymbol{PA}' + \boldsymbol{Q}\right) \boldsymbol{x} = \mathbf{0}. \tag{23}$$

Therefore, the Riccati equation (17) must be solved in order to find $\boldsymbol{P} > 0$, which concludes the proof. ■

Remark 3: Theorem 1 demonstrates that a solution to the optimal nonlinear $\mathcal{W}_\infty$ control problem (7), governed by the HJ PDE (15), for the nonautonomous nonlinear dynamical system (5) can be provided by the constant quadratic function (16). Similar solutions of optimal nonlinear control problems are found in the literature for nonlinear nonautonomous mechanical systems [24], [25], [26].

Remark 4: The optimal control law (13), derived from (7) and applied to the nonlinear system (5), transforms the closed-loop dynamics (22) into an autonomous linear system.

Theorem 2: Given that Assumptions 1 and 2 hold. Let $\boldsymbol{q}_r(t) \in \mathcal{C}^3$ and V be a solution of (15) given by the parameterized scalar function (16). Therefore, the closed-loop system, formed by the control law (13) and system (5), is asymptotically stable within the configuration domain Ω.

Proof: From (16), we have that $V > 0$, $\forall \boldsymbol{x} \neq 0$, and from (18), we obtain

$$\frac{\partial V}{\partial \boldsymbol{x}} \dot{\boldsymbol{x}} = -\frac{1}{2} \begin{bmatrix} \boldsymbol{x} \\ \dddot{\tilde{q}} \end{bmatrix}' \begin{bmatrix} \mathbf{\Gamma}_0 & \mathbf{0} & \mathbf{0} & \mathbf{0} & \mathbf{0} \\ \mathbf{0} & \mathbf{\Gamma}_1 & \mathbf{0} & \mathbf{0} & \mathbf{0} \\ \mathbf{0} & \mathbf{0} & \mathbf{\Gamma}_2 & \mathbf{0} & \mathbf{0} \\ \mathbf{0} & \mathbf{0} & \mathbf{0} & \mathbf{\Gamma}_3 & \mathbf{0} \\ \mathbf{0} & \mathbf{0} & \mathbf{0} & \mathbf{0} & \mathbf{\Gamma}_4 \end{bmatrix} \begin{bmatrix} \boldsymbol{x} \\ \dddot{\tilde{q}} \end{bmatrix} < \mathbf{0}. \tag{24}$$

Therefore, (16) is a Lyapunov function that ensures asymptotic stability to the closed-loop system. ■

III. GENERALIZED APPROACH

The approach previously presented can be generalized for any number of time derivatives. Therefore, taking into account (1), the n-th time derivative of $\boldsymbol{q}(t)$ is given by

$$\begin{aligned} \overset{(n)}{\boldsymbol{q}}(t) &= \boldsymbol{h}_{(n)}(\boldsymbol{q}, \cdots, \overset{(n-1)}{\boldsymbol{q}}, \boldsymbol{u}, \cdots, \overset{(n-3)}{\boldsymbol{u}}, t) \\ &+ \boldsymbol{G}_{(n)}(\boldsymbol{q}, \cdots, \overset{(n-2)}{\boldsymbol{q}}, \boldsymbol{u}, \cdots, \overset{(n-3)}{\boldsymbol{u}}, t) \overset{(n-2)}{\boldsymbol{u}} + \overset{(n-2)}{\boldsymbol{w}}, \end{aligned} \tag{25}$$

where $\boldsymbol{h}_{(n)}(\boldsymbol{q}, \cdots, \overset{(n-1)}{\boldsymbol{q}}, \boldsymbol{u}, \cdots, \overset{(n-3)}{\boldsymbol{u}}, t)$ and $\boldsymbol{G}_{(n)}(\boldsymbol{q}, \cdots, \overset{(n-2)}{\boldsymbol{q}}, \boldsymbol{u}, \cdots, \overset{(n-3)}{\boldsymbol{u}}, t)$ are computed following a similar procedure used to obtain (3).

Hence, considering the state vector

$$\boldsymbol{x}(t) \triangleq \begin{bmatrix} (\int_0^t \tilde{\boldsymbol{q}}(\tau) d\tau)' & \tilde{\boldsymbol{q}}' & \dot{\tilde{\boldsymbol{q}}}' & \cdots & (\overset{(n-1)}{\tilde{\boldsymbol{q}}})' \end{bmatrix}', \tag{26}$$

with $\boldsymbol{q}_r \in \mathcal{C}^n$, the tracking error dynamics can be represented in the state-space as follows

$$\dot{\boldsymbol{x}} = \overbrace{\begin{bmatrix} \mathbf{0} & \boldsymbol{I} \\ \mathbf{0} & \mathbf{0} \end{bmatrix} \boldsymbol{x} + \begin{bmatrix} \mathbf{0} \\ \boldsymbol{h}_{(n)} \end{bmatrix}}^{\bar{\boldsymbol{h}}} + \overbrace{\begin{bmatrix} \mathbf{0} \\ \boldsymbol{G}_{(n)} \end{bmatrix}}^{\bar{\boldsymbol{G}}} \overset{(n-2)}{\boldsymbol{u}} + \overbrace{\begin{bmatrix} \mathbf{0} \\ \boldsymbol{I} \end{bmatrix}}^{\bar{\boldsymbol{K}}} \overset{(n-2)}{\boldsymbol{w}}, \tag{27}$$

and placed in the standard form (5). Then, inequality (6) is generalized as

$$||\boldsymbol{z}(t)||_{\mathcal{W}_{(n+1),2,\Gamma}} \leq \gamma || \overset{(n-2)}{\boldsymbol{w}}(t) ||_{\mathcal{L}_2}, \tag{28}$$

for any $\overset{(n-2)}{\boldsymbol{w}}(t) \in \mathcal{L}_2$ and with $\boldsymbol{z}(t) \triangleq \int_0^t \tilde{\boldsymbol{q}}(\tau) d\tau$. Accordingly, the robust nonlinear $\mathcal{W}_\infty$ OCP is posed as

$$\min_{\overset{(n-2)}{\boldsymbol{u}} \in \mathcal{U}} \max_{\overset{(n-2)}{\boldsymbol{w}} \in \mathcal{L}_2} \frac{1}{2} ||\boldsymbol{z}(t)||^2_{\mathcal{W}_{(n+1),2,\Gamma}} - \frac{1}{2} \gamma^2 || \overset{(n-2)}{\boldsymbol{w}}(t) ||^2_{\mathcal{L}_2}. \tag{29}$$

Remark 5: Assumptions 1 and 2 hold, similarly, for (27).

Similar to the approach presented in Section II, we consider $V(\boldsymbol{x}) = \boldsymbol{x}'\boldsymbol{P}\boldsymbol{x}$ to formulate (7) using dynamic programming, which leads to the optimal control law

$$\overset{(n-2)}{\boldsymbol{u}}{}^* = -\left(\boldsymbol{G}'_{(n)} \mathbf{\Gamma}_{(n+1)} \boldsymbol{G}_{(n)}\right)^{-1} \left(\bar{\boldsymbol{G}}' \boldsymbol{P}\boldsymbol{x} + \boldsymbol{G}'_{(n)} \mathbf{\Gamma}_{(n+1)} \boldsymbol{h}\right), \tag{30}$$

with matrix $\boldsymbol{P} > 0$ obtained from the solution of the Riccati equation

$$-\boldsymbol{P}\bar{\boldsymbol{B}}\boldsymbol{P} + \bar{\boldsymbol{A}}\boldsymbol{P} + \boldsymbol{P}\bar{\boldsymbol{A}}' + \bar{\boldsymbol{Q}} = \mathbf{0}, \tag{31}$$

and

$$\bar{\boldsymbol{A}} \triangleq \begin{bmatrix} \mathbf{0} & \boldsymbol{I} \\ \mathbf{0} & \mathbf{0} \end{bmatrix}, \bar{\boldsymbol{B}} \triangleq \begin{bmatrix} \mathbf{0} & \mathbf{0} \\ \mathbf{0} & \mathbf{\Gamma}_{(n+1)}^{-1} \end{bmatrix}, \bar{\boldsymbol{Q}} \triangleq \text{blkdiag}(\mathbf{\Gamma}_0, \cdots, \mathbf{\Gamma}_{(n-1)})$$

Theorem 3: Given that Assumptions 1 and 2 hold. Let $\boldsymbol{q}_r \in \mathcal{C}^n$ and $\boldsymbol{P} > 0$ be a solution of (31). Therefore, the closed-loop system, formed by the control law (30) and system (27), is asymptotically stable within the configuration domain Ω.

Proof: This proof can be deduced in a similar manner to the proof of Theorem 2. ■

Remark 6: If the system described by (1) is already input affine, it can be expressed by (25) with $n = 2$. Furthermore, the solution of the OCP (7) using dynamic programming for that system also results in an optimal control law that takes the form of (30).

IV. APPLICATION TO A QUADROTOR

In this section, we design a control strategy based on the proposed nonlinear $\mathcal{W}_\infty$ control method for trajectory tracking of a quadrotor. Due to the dynamical model structure of the quadrotor, we can split it into two interconnected subsystems: the rotational and the translational. Since these subsystems can be arranged in a cascade form, the control inputs of translational dynamics are used as reference in the rotational control loop. As detailed below, the translational dynamics are nonaffine on the control inputs, whereas the rotational dynamics are affine on their control inputs. This highlights the versatility of the proposed method in designing both inner and outer controllers.

Consider the quadrotor dynamics described by the Euler-Lagrange equation in the canonical form [27]

$$\boldsymbol{M}(\boldsymbol{q})\ddot{\boldsymbol{q}} + \boldsymbol{C}(\boldsymbol{q}, \dot{\boldsymbol{q}})\dot{\boldsymbol{q}} + \boldsymbol{g}(\boldsymbol{q}) = \boldsymbol{B}(\boldsymbol{q})\boldsymbol{\tau} + \boldsymbol{w}, \tag{32}$$

with

$$\begin{aligned} &\boldsymbol{q} \triangleq [\phi\ \theta\ \psi\ x\ y\ z]', \boldsymbol{w} \triangleq [\delta_\phi\ \delta_\theta\ \delta_\psi\ \delta_x\ \delta_y\ \delta_z]', \\ &\boldsymbol{\tau} \triangleq [\tau_\phi\ \tau_\theta\ \tau_\psi\ f_z]', \boldsymbol{g}(\boldsymbol{q}) \triangleq \begin{bmatrix} \mathbf{0} & mg\boldsymbol{a}_z' \end{bmatrix}', \\ &\boldsymbol{M}(\boldsymbol{q}) \triangleq \begin{bmatrix} \boldsymbol{\mathcal{W}}_\eta' \mathbb{I} \boldsymbol{\mathcal{W}}_\eta & \mathbf{0} \\ \mathbf{0} & m\boldsymbol{I} \end{bmatrix}, \boldsymbol{B}(\boldsymbol{q}) \triangleq \begin{bmatrix} \boldsymbol{\mathcal{W}}_\eta' & \mathbf{0} \\ \mathbf{0} & \boldsymbol{R}\boldsymbol{a}_z \end{bmatrix}, \end{aligned}$$

$$\boldsymbol{\mathcal{W}}_\eta \triangleq \begin{bmatrix} 1 & 0 & -\sin(\theta) \\ 0 & \cos(\phi) & \sin(\phi)\cos(\theta) \\ 0 & -\sin(\phi) & \cos(\phi)\cos(\theta) \end{bmatrix},$$

where $\boldsymbol{q}(t) : \mathbb{R}_{\geq 0} \to \mathbb{R}^6$ stands for the vector of generalized coordinates, $\boldsymbol{a}_z \triangleq \begin{bmatrix} 0 & 0 & 1 \end{bmatrix}'$, $\boldsymbol{R} \in SO(3)$ with $\boldsymbol{R} \triangleq \boldsymbol{R}_{z,\psi}\boldsymbol{R}_{y,\theta}\boldsymbol{R}_{x,\phi}$, in which ϕ, θ and ψ stand for the quadrotor orientation using Euler angles, with roll-pitch-yaw convention, where $\boldsymbol{R}_{x,\phi}$, $\boldsymbol{R}_{y,\theta}$, and $\boldsymbol{R}_{z,\psi}$ denote rotation matrices of angles ϕ, θ, and ψ around $\vec{x}$, $\vec{y}$, and $\vec{z}$ axes, respectively; x, y and z describe the three-dimensional translational position of the quadrotor; f_z, τ_ϕ, τ_θ, and τ_ψ are the total thrust and the torques applied on the roll, pitch, and yaw motions, respectively; δ_ϕ, δ_θ, δ_ψ, δ_x, δ_y, and δ_z are generalized external disturbances; m is the quadrotor's mass; g is the magnitude of the gravitational acceleration; and $\mathbb{I} \triangleq \text{diag}(I_{xx}, I_{yy}, I_{zz})$ is the quadrotor inertia tensor matrix. The Coriolis and centrifugal force matrix, $\boldsymbol{C}(\boldsymbol{q}, \dot{\boldsymbol{q}})$, can be obtained from the Christoffel symbols of the first kind, as

$$\boldsymbol{C}_{k,j} = \sum_{l=1}^{8} \frac{1}{2} \left[\partial \boldsymbol{M}_{k,j}/\partial \boldsymbol{q}_l + \partial \boldsymbol{M}_{k,l}/\partial \boldsymbol{q}_j - \partial \boldsymbol{M}_{l,j}/\partial \boldsymbol{q}_k\right] \dot{\boldsymbol{q}}_l,$$

where $\boldsymbol{C}_{k,j}$ and $\boldsymbol{M}_{k,j}$ are elements of the Coriolis and inertia matrices, respectively, corresponding to the k-th row and j-th column. The quadrotor physical parameters are $I_{xx} = 0.0363$, Kg.m^2 $I_{yy} = 0.0363$ Kg.m^2, $I_{zz} = 0.0615$ Kg.m^2, $m = 2.2$ Kg, and $g = 9.8$ m/s^2.

Assumption 3: The quadrotor's vector of generalized coordinates, $\boldsymbol{q}(t)$, and its time derivative, $\dot{\boldsymbol{q}}(t)$, are available for control design purposes.

To design the cascade control strategy for the quadrotor, we can split the equations of motion (32) regarding the rotational and translational dynamics as follows

$$\begin{bmatrix} \boldsymbol{M}_{ii} & \boldsymbol{0} \\ \boldsymbol{0} & \boldsymbol{M}_{oo} \end{bmatrix}\begin{bmatrix} \ddot{\boldsymbol{q}}_i \\ \ddot{\boldsymbol{q}}_o \end{bmatrix} + \begin{bmatrix} \boldsymbol{C}_{ii} & \boldsymbol{C}_{io} \\ \boldsymbol{C}_{oi} & \boldsymbol{C}_{oo} \end{bmatrix}\begin{bmatrix} \dot{\boldsymbol{q}}_i \\ \dot{\boldsymbol{q}}_o \end{bmatrix} + \begin{bmatrix} \boldsymbol{g}_i \\ \boldsymbol{g}_o \end{bmatrix} = \begin{bmatrix} \boldsymbol{B}_i \\ \boldsymbol{B}_o \end{bmatrix}\boldsymbol{\tau} + \begin{bmatrix} \boldsymbol{w}_i \\ \boldsymbol{w}_o \end{bmatrix}, \quad (33)$$

where $\boldsymbol{q}_i(t) : \mathbb{R}_{\geq 0} \to \mathbb{R}^3$, with $\boldsymbol{q}_i(t) \triangleq [\phi\ \theta\ \psi]'$ being the inner-loop degrees of freedom (DOF), and $\boldsymbol{q}_o(t) : \mathbb{R}_{\geq 0} \to \mathbb{R}^{n_o}$, with $\boldsymbol{q}_o(t) \triangleq [x\ y\ z]'$ the outer-loop DOF. Hence, from the first row of (33), the tracking error dynamics of the inner-loop DOF are given by

$$\begin{aligned} \ddot{\tilde{\boldsymbol{q}}}_i &= -\boldsymbol{M}_{ii}^{-1}\left(\begin{bmatrix} \boldsymbol{C}_{ii} & \boldsymbol{C}_{io} \end{bmatrix}\dot{\boldsymbol{q}} + \boldsymbol{g}_i\right) - \ddot{\boldsymbol{q}}_{i_r} + \boldsymbol{M}_{ii}^{-1}\left(\boldsymbol{B}_i\boldsymbol{\tau} + \boldsymbol{w}_i\right), \\ &= \overbrace{-\boldsymbol{M}_{ii}^{-1}\boldsymbol{C}_{ii}\dot{\boldsymbol{q}}_i - \ddot{\boldsymbol{q}}_{i_r}}^{\boldsymbol{h}_{(2)}(\boldsymbol{q}_i, \dot{\boldsymbol{q}}_i, t)} + \overbrace{\boldsymbol{M}_{ii}^{-1}\boldsymbol{B}_i}^{G_{(2)}(\boldsymbol{q}_i)}\boldsymbol{\tau}_i + \overbrace{\boldsymbol{M}_{ii}^{-1}\boldsymbol{w}_i}^{\bar{\boldsymbol{w}}_i}, \\ &= \boldsymbol{h}_{(2)}(\boldsymbol{q}_i, \dot{\boldsymbol{q}}_i, t) + G_{(2)}(\boldsymbol{q}_i)\boldsymbol{\tau}_i + \bar{\boldsymbol{w}}_i, \end{aligned} \quad (34)$$

where $\boldsymbol{\tau}_i \triangleq [\tau_\phi\ \ \tau_\theta\ \ \tau_\psi]'$, $\bar{\boldsymbol{w}}_i \triangleq \boldsymbol{M}_{ii}^{-1}\boldsymbol{w}_1$, and $\boldsymbol{q}_{i_r}(t) \in \mathcal{C}^2$ stands for the desired references of the inner-loop DOF. It is worth mentioning that $\boldsymbol{C}_{io} = \boldsymbol{0}$, $\boldsymbol{g}_i = \boldsymbol{0}$, and the matrices are independent of $\boldsymbol{q}_o$ and $\dot{\boldsymbol{q}}_o$. Then, considering the state vector

$$\boldsymbol{x}_i(t) \triangleq \left[(\textstyle\int_0^t \tilde{\boldsymbol{q}}_i(\tau)d\tau)' \quad \tilde{\boldsymbol{q}}_i' \quad \dot{\tilde{\boldsymbol{q}}}_i'\right]', \quad (35)$$

and the cost variable $\boldsymbol{z}_i(t) = \int_0^t \tilde{\boldsymbol{q}}_i(\tau)d\tau$, the control input affine system (34) can be represented in the state-space form (27), with $n = 2$. For that system, the OCP (7) is posed and, from its solution via dynamic programming, the optimal control law (30) is obtained. Thus, the optimal control law provides trajectory tracking of a desired reference given by $\boldsymbol{q}_{i_r}(t)$, $\dot{\boldsymbol{q}}_{i_r}(t)$, and $\ddot{\boldsymbol{q}}_{i_r}(t)$, ensuring asymptotic stability to the inner closed-loop system, i.e. $\lim_{t\to\infty} \boldsymbol{x}_i(t) = \boldsymbol{0}$. It is worth noting that, considering the interconnected cascade controller, the desired values of $\phi_r(t)$ and $\theta_r(t)$ come from the outer-loop controller.

To design the outer-loop controller, initially, from the second row of (33), we obtain

$$\begin{aligned} \ddot{\boldsymbol{q}}_o &= -\boldsymbol{M}_{oo}^{-1}\left(\begin{bmatrix} \boldsymbol{C}_{oi} & \boldsymbol{C}_{oo} \end{bmatrix}\dot{\boldsymbol{q}} + \boldsymbol{g}_o\right) + \boldsymbol{M}_{oo}^{-1}\left(\boldsymbol{B}_o\boldsymbol{\tau} + \boldsymbol{w}_o\right), \\ &= \overbrace{-g\boldsymbol{a}_z + \frac{1}{m}\boldsymbol{R}\boldsymbol{a}_z f_z}^{\boldsymbol{f}(\psi, \boldsymbol{u})} + \overbrace{\frac{1}{m}\boldsymbol{w}_o}^{\bar{\boldsymbol{w}}_o}, \end{aligned} \quad (36)$$

where $\boldsymbol{C}_{oi} = \boldsymbol{C}_{oo} = \boldsymbol{0}$. Let us assume the yaw angle as a time-varying parameter equal to its reference, $\psi_r(t)$, which is tracked by the inner-loop controller. Thus, the remaining variables we can manipulate are the total thrust, f_z, as well as the roll and pitch angles. However, the latter are also controlled in the inner-loop. Consequently, instead of manipulating ϕ and θ, for control design purposes we manipulate their references, ϕ_r, θ_r. For consistency of notation, we also set $f_z = f_{z_r}$. Accordingly, we can write system (36) as the control input nonaffine nonlinear system

$$\ddot{\boldsymbol{q}}_o = \boldsymbol{f}(\psi_r, \boldsymbol{u}, t) + \bar{\boldsymbol{w}}_o(t), \quad (37)$$

with $\bar{\boldsymbol{w}}_o \triangleq \dfrac{1}{m}\boldsymbol{w}_o$ and $\boldsymbol{u} \triangleq [\phi_r\ \theta_r\ f_{z_r}]'$.

As the inner-loop controller requires the desired reference $\boldsymbol{q}_{i_r}(t) \in \mathcal{C}^2$, the outer-loop control law must be given in terms of the second-time derivative of $\phi_r(t)$ and $\theta_r(t)$. Therefore, we increase the order of (37) to obtain an input affine function of $\ddot{\boldsymbol{u}}$. Hence, the third time derivative of $\tilde{\boldsymbol{q}}_o$ is computed as

$$\dddot{\boldsymbol{q}}_o = \frac{\partial \boldsymbol{f}}{\partial \psi_r}\dot{\psi}_r + \frac{\partial \boldsymbol{f}}{\partial \boldsymbol{u}}\dot{\boldsymbol{u}} + \dot{\bar{\boldsymbol{w}}}_o = \boldsymbol{f}_{(3)}(\psi_r, \dot{\psi}_r, \boldsymbol{u}, \dot{\boldsymbol{u}}), \quad (38)$$

while the fourth time derivative of $\dddot{\boldsymbol{q}}_o$ is given by

$$\ddddot{\boldsymbol{q}}_o = \begin{bmatrix} \dfrac{\partial \boldsymbol{f}_{(3)}}{\partial \psi_r} & \dfrac{\partial \boldsymbol{f}_{(3)}}{\partial \dot{\psi}_r} & \dfrac{\partial \boldsymbol{f}_{(3)}}{\partial \boldsymbol{u}} \end{bmatrix}\begin{bmatrix} \dot{\psi}_r \\ \ddot{\psi}_r \\ \dot{\boldsymbol{u}} \end{bmatrix} + \frac{\partial \boldsymbol{f}_{(3)}}{\partial \dot{\boldsymbol{u}}}\ddot{\boldsymbol{u}} + \ddot{\bar{\boldsymbol{w}}}_o. \quad (39)$$

From (39), the tracking error dynamics of the outer-loop DOF can be written as

$$\ddddot{\tilde{\boldsymbol{q}}}_o = \boldsymbol{h}_{(4)}(\psi_r, \dot{\psi}_r, \ddot{\psi}_r, \boldsymbol{u}, \dot{\boldsymbol{u}}, t) + \boldsymbol{G}_{(4)}(\psi_r, \dot{\psi}_r, \boldsymbol{u}, \dot{\boldsymbol{u}})\ddot{\boldsymbol{u}} + \ddot{\bar{\boldsymbol{w}}}_o, \quad (40)$$

with $\boldsymbol{h}_{(4)} \triangleq \begin{bmatrix} \dfrac{\partial \boldsymbol{f}_{(3)}}{\partial \psi_r} & \dfrac{\partial \boldsymbol{f}_{(3)}}{\partial \dot{\psi}_r} & \dfrac{\partial \boldsymbol{f}_{(3)}}{\partial \boldsymbol{u}} \end{bmatrix}\begin{bmatrix} \dot{\psi}_r \\ \ddot{\psi}_r \\ \dot{\boldsymbol{u}} \end{bmatrix} - \ddddot{\boldsymbol{q}}_{o_r}$ and $\boldsymbol{G}_{(4)} \triangleq \dfrac{\partial \boldsymbol{f}_{(3)}}{\partial \dot{\boldsymbol{u}}}$, where $\boldsymbol{q}_{o_r} \in \mathcal{C}^4$ stands for the desired references to the inner-loop DOF.

Taking into account the state vector

$$\boldsymbol{x}_o(t) \triangleq \left[(\textstyle\int_0^t \tilde{\boldsymbol{q}}_o(\tau)d\tau)' \quad \tilde{\boldsymbol{q}}_o' \quad \dot{\tilde{\boldsymbol{q}}}_o' \quad \ddot{\tilde{\boldsymbol{q}}}_o' \quad \dddot{\tilde{\boldsymbol{q}}}_o'\right]', \quad (41)$$

and the cost variable $\boldsymbol{z}_o(t) = \int_0^t \tilde{\boldsymbol{q}}_o(\tau)d\tau$, the system (40) can be represented in the state-space form (27), with $n = 4$. For that system, the OCP (7) is posed and, from its solution via dynamic programming, the optimal control law (30) is obtained. This optimal control law generates desired references that, when tracked, asymptotically stabilize the outer-loop system such that $\lim_{t\to\infty} \boldsymbol{x}_o(t) = \boldsymbol{0}$.

Let us proceed with the stability analysis of the whole closed-loop. As commented, the asymptotic stability of the inner-loop control system is guaranteed by Theorem 2, i.e. $\lim_{t\to\infty} \boldsymbol{x}_i(t) = \boldsymbol{0}$. For the outer-loop system, its tracking error dynamics are written in terms of the fourth time derivative of $\boldsymbol{q}_o$, leading to

$$\ddddot{\boldsymbol{q}}_o=\boldsymbol{h}_{(4)}(\psi,\dot{\psi},\ddot{\psi},\bar{\boldsymbol{u}},\dot{\bar{\boldsymbol{u}}},t)+\boldsymbol{G}_{(4)}(\psi,\dot{\psi},\bar{\boldsymbol{u}},\dot{\bar{\boldsymbol{u}}})\ddot{\bar{\boldsymbol{u}}}+\ddot{\boldsymbol{w}}_o, \quad (42)$$

which is given by using the same notation as in (36), and $\bar{\boldsymbol{u}} \triangleq [\phi \;\; \theta \;\; f_z]'$. Hence, by manipulating (42) as follows

$$\begin{aligned}\ddddot{\boldsymbol{q}}_o=&\boldsymbol{h}_{(4)}(\psi,\dot{\psi},\ddot{\psi},\bar{\boldsymbol{u}},\dot{\bar{\boldsymbol{u}}},t)+\boldsymbol{G}_{(4)}(\psi,\dot{\psi},\bar{\boldsymbol{u}},\dot{\bar{\boldsymbol{u}}})\ddot{\bar{\boldsymbol{u}}}+\ddot{\boldsymbol{w}}_o\\ &+\boldsymbol{h}_{(4)}(\psi_r,\dot{\psi}_r,\ddot{\psi}_r,\boldsymbol{u},\dot{\boldsymbol{u}},t)+\boldsymbol{G}_{(4)}(\psi_r,\dot{\psi}_r,\boldsymbol{u},\dot{\boldsymbol{u}})\ddot{\boldsymbol{u}}\\ &-\boldsymbol{h}_{(4)}(\psi_r,\dot{\psi}_r,\ddot{\psi}_r,\boldsymbol{u},\dot{\boldsymbol{u}},t)-\boldsymbol{G}_{(4)}(\psi_r,\dot{\psi}_r,\boldsymbol{u},\dot{\boldsymbol{u}})\ddot{\boldsymbol{u}},\end{aligned} \quad (43)$$

we obtain

$$\ddddot{\boldsymbol{q}}_o=\boldsymbol{h}_{(4)}(\psi_r,\dot{\psi}_r,\ddot{\psi}_r,\boldsymbol{u},\dot{\boldsymbol{u}},t)+\boldsymbol{G}_{(4)}(\psi_r,\dot{\psi}_r,\boldsymbol{u},\dot{\boldsymbol{u}})\ddot{\boldsymbol{u}}+\ddot{\bar{\boldsymbol{w}}}_o, \quad (44)$$

in which $\ddot{\bar{\boldsymbol{w}}}_o \triangleq \vartheta(\boldsymbol{\eta}) - \vartheta(\boldsymbol{\eta}_r) + \ddot{\boldsymbol{w}}_o$, where $\vartheta(\boldsymbol{\eta}) \triangleq \boldsymbol{h}_{(4)}(\psi,\dot{\psi},\ddot{\psi},\bar{\boldsymbol{u}},\dot{\bar{\boldsymbol{u}}},t) + \boldsymbol{G}_{(4)}(\psi,\dot{\psi},\bar{\boldsymbol{u}},\dot{\bar{\boldsymbol{u}}})\ddot{\bar{\boldsymbol{u}}}$, and $\vartheta(\boldsymbol{\eta}_r) \triangleq \boldsymbol{h}_{(4)}(\psi_r,\dot{\psi}_r,\ddot{\psi}_r,\boldsymbol{u},\dot{\boldsymbol{u}},t) + \boldsymbol{G}_{(4)}(\psi_r,\dot{\psi}_r,\boldsymbol{u},\dot{\boldsymbol{u}})\ddot{\boldsymbol{u}}$, with $\boldsymbol{\eta} \triangleq [\boldsymbol{q}_i' \;\; \dot{\boldsymbol{q}}_i' \;\; \ddot{\boldsymbol{q}}_i' \;\; f_z \;\; \dot{f}_z \;\; \ddot{f}_z]'$ and $\boldsymbol{\eta}_r \triangleq [\boldsymbol{q}_{i_r}' \;\; \dot{\boldsymbol{q}}_{i_r}' \;\; \ddot{\boldsymbol{q}}_{i_r}' \;\; f_{z_r} \;\; \dot{f}_{z_r} \;\; \ddot{f}_{z_r}]'$. Assuming that $\ddot{\bar{\boldsymbol{w}}}_o$ represents the disturbance vector for the outer-loop dynamics, the stability analysis of system (44) interconnected with the inner-loop system can be performed in the following manner.

If no disturbances act on (44), i.e. $\ddot{\bar{\boldsymbol{w}}}_o = \boldsymbol{0}$, the control law $\ddot{\boldsymbol{u}}$ obtained from the solution of the OCP (29), with $n = 4$, ensures asymptotic stability of the closed-loop system, as proven in Theorem 3. On the other hand, if $\ddot{\bar{\boldsymbol{w}}}_o \neq \boldsymbol{0}$, the asymptotic stability of the outer-loop system can still be guaranteed if $\ddot{\bar{\boldsymbol{w}}}_o \in \mathcal{L}_2$. It is worth mentioning that, by the construction of the control problem (29), the control law $\ddot{\boldsymbol{u}}$ ensures that the inequality $||\boldsymbol{z}_o(t)||_{\mathcal{W}_{5,2,\Gamma}} \leq \gamma||\ddot{\bar{\boldsymbol{w}}}_o(t)||_{\mathcal{L}_2}$ holds (see (28)). Therefore, to demonstrate that $\ddot{\bar{\boldsymbol{w}}}_o \in \mathcal{L}_2$, it is necessary to establish that $(\vartheta(\boldsymbol{\eta}) - \vartheta(\boldsymbol{\eta}_r)) \in \mathcal{L}_2$, given that $\ddot{\boldsymbol{w}}_o \in \mathcal{L}_2$ by assumption of the control problem. To do so, it is noted that functions $\boldsymbol{h}_{(4)}$ and $\boldsymbol{G}_{(4)}$ are Lipschitz continuous, implying the existence of a constant $k \in \mathbb{R}_{>0}$, such that

$$||\vartheta(\boldsymbol{\eta}) - \vartheta(\boldsymbol{\eta}_r)||_2 \leq k||\boldsymbol{\eta} - \boldsymbol{\eta}_r||_2 \quad (45)$$

holds. Then, by integrating both sides of (45) leads to

$$\begin{aligned}\lim_{t\to\infty}\int_0^t ||\vartheta(\boldsymbol{\eta}) - \vartheta(\boldsymbol{\eta}_r)||_2 dt &\leq k \lim_{t\to\infty}\int_0^t ||\boldsymbol{\eta} - \boldsymbol{\eta}_r||_2 dt,\\ &\leq k||\boldsymbol{\eta} - \boldsymbol{\eta}_r||_{\mathcal{L}_2}.\end{aligned} \quad (46)$$

Therefore, the stability analysis can be demonstrated by defining $\tilde{\boldsymbol{\eta}} \triangleq \boldsymbol{\eta} - \boldsymbol{\eta}_r$, and showing that each element in $\tilde{\boldsymbol{\eta}}$ belongs to the $\mathcal{L}_2$ space. It is true that $\left(\tilde{\boldsymbol{\eta}} \in \mathcal{L}_2 \implies \ddot{\bar{\boldsymbol{w}}}_o \in \mathcal{L}_2\right)$, making it sufficient to demonstrate the former. Firstly, since f_z is a control input of system (32), it can be applied exactly, ensuring $||\tilde{f}_z||_{\mathcal{L}_2} = 0$, $||\dot{\tilde{f}}_z||_{\mathcal{L}_2} = 0$, and $||\ddot{\tilde{f}}_z||_{\mathcal{L}_2} = 0$, with $\tilde{f}_z \triangleq f_z - f_{z_r}$. Furthermore, the inner-loop controller ensures $||\boldsymbol{z}_i(t)||_{\mathcal{W}_{3,2,\Gamma}} \leq \gamma||\boldsymbol{w}_i(t)||_{\mathcal{L}_2}$, which implies $||\tilde{q}_i||_{\mathcal{L}_2} < \infty$, $||\dot{\tilde{q}}_i||_{\mathcal{L}_2} < \infty$, and $||\ddot{\tilde{q}}_i||_{\mathcal{L}_2} < \infty$ for any $\boldsymbol{w}_i \in \mathcal{L}_2$, which concludes the stability analysis of the interconnected cascade control system.

A. Numerical Results

Numerical experiment results are presented here to corroborate the efficacy of the proposed control strategy.

In order to implement the optimal control law (30) with state vector (41), Assumption 3 must hold. Therefore, the numerical experiment is here conducted by estimating the vectors $\ddot{\boldsymbol{q}}_o$ and $\dddot{\boldsymbol{q}}_o$, as follows

$$\ddot{\boldsymbol{q}}_o = -g\boldsymbol{a}_z + \frac{1}{m}\boldsymbol{R}\boldsymbol{a}_z f_{z_r}, \quad (47)$$

$$\dddot{\boldsymbol{q}}_o = \frac{1}{m}\dot{\boldsymbol{R}}\boldsymbol{a}_z f_{z_r} + \frac{1}{m}\boldsymbol{R}\boldsymbol{a}_z \dot{f}_{z_r}, \quad (48)$$

with $\bar{\boldsymbol{R}} \triangleq \boldsymbol{R}_{z,\psi_r}\boldsymbol{R}_{y,\theta_r}\boldsymbol{R}_{x,\phi_r}$.

To verify the tracking capabilities of the proposed nonlinear $\mathcal{W}_\infty$ controller, the quadrotor is designated to perform the desired trajectory $x_r(t) = 12\cos(2\pi t/40)$, $y_r(t) = 12\sin(2\pi t/20)$, $z(t) = 10 - 3\cos(2\pi t/40)$, and $\psi(t) = 0$, while subjected to the disturbances illustrated in Fig. 1, starting from the initial position $\boldsymbol{q}(0) = [1\ 0\ 1\ \ 11\ \ 0\ 0]'$.

The quadrotor was displaced from the desired trajectory at the beginning of the numerical experiment. It converged to the trajectory, remaining on it until the disturbances δ_y and δ_θ were applied to the system. To attenuate the effects of δ_y, the outer-loop controller manipulated the nonaffine inputs $\boldsymbol{u}$ in (37), i.e., it tilted the quadrotor with respect to the ϕ angle generating a physical projection of the slightly increased total thrust f_z. Also, to attenuate the effects of δ_θ, the inner-loop controller manipulated the affine control input τ_θ in (34). Accordingly, the outer-loop controller effectively handled the nonaffine inputs and, in conjunction with the inner-loop controller, achieved trajectory tracking with asymptotic stability for the whole closed-loop system while mitigating the impact of external disturbances. These findings are consistent with the theoretical framework presented in this study.

V. CONCLUSIONS

We proposed a novel robust nonlinear $\mathcal{W}_\infty$ optimal control approach for control input nonaffine, nonautonomous dynamical system, aiming to solve the trajectory tracking problem. The proposed control approach was developed by considering a weighted Sobolev, $\mathcal{W}_{m,p,\Gamma}$, norm, of the cost variable, with the goal of enhancing transient performance. The OCP was formulated via dynamic programming, addressing increased-order systems with any number of time derivatives. A particular solution to the resulting HJ equation was proposed, along with the corresponding demonstration of asymptotic stability. The theoretical framework was corroborated by a numerical experiment. By employing the proposed approach, we designed an interconnected cascade controller for a quadrotor, ensuring trajectory tracking with guaranteed asymptotic stability of the whole closed-loop system. In future work, we intend to formulate the dynamic output feedback robust nonlinear $\mathcal{W}_\infty$ controller for input nonaffine dynamical systems.

REFERENCES

[1] X. Shi, K. Kim, S. Rahili, and S.-J. Chung, "Nonlinear control of autonomous flying cars with wings and distributed electric propulsion," in *IEEE Conference on Decision and Control*, 2018, pp. 5326–5333.

[2] T. D. Son and Q. Nguyen, "Safety-critical control for non-affine nonlinear systems with application on autonomous vehicle," in *IEEE Conference on Decision and Control*, 2019, pp. 7623–7628.

[3] O. Alshammari, M. N. Mahyuddin, and H. Jerbi, "A neural network-based adaptive backstepping control law with covariance resetting for asymptotic output tracking of a cstr plant," *IEEE Access*, vol. 8, pp. 29 755–29 766, 2020.

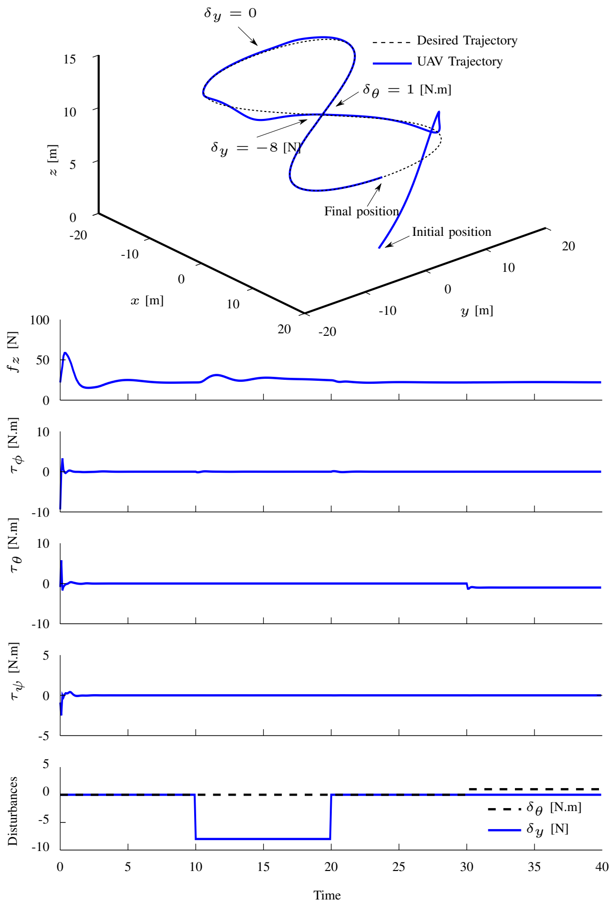

Fig. 1. 3D visualization of the trajectory tracking over time, with the applied control inputs and disturbance.

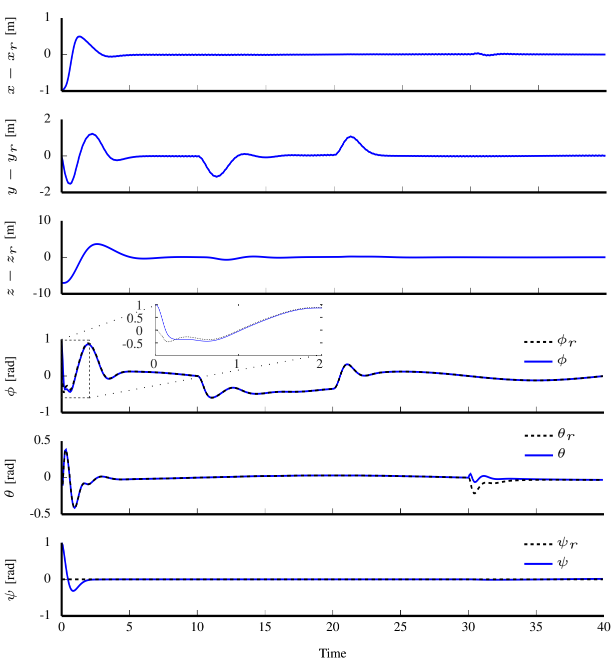

Fig. 2. Plot illustrating the outer-loop degree-of-freedom (DOF) trajectory tracking error, alongside the time evolution of the inner-loop DOF and their respective desired references.

[4] H. Nijmeijer and A. Van der Schaft, *Nonlinear dynamical control systems*. Springer, 1990, vol. 175.

[5] S.-L. Dai, C. Wang, and M. Wang, "Dynamic learning from adaptive neural network control of a class of nonaffine nonlinear systems," *IEEE transactions on neural networks and learning systems*, vol. 25, no. 1, pp. 111–123, 2013.

[6] J. D. Boskovic, L. Chen, and R. K. Mehra, "Adaptive control design for nonaffine models arising in flight control," *Journal of guidance, control, and dynamics*, vol. 27, no. 2, pp. 209–217, 2004.

[7] J. Medrano, F. Yumbla, S. Jeong, I. Choi, Y. Park, E. Auh, and H. Moon, "Jerk estimation for quadrotor based on differential flatness," in *2020 17th International Conference on Ubiquitous Robots (UR)*. IEEE, 2020, pp. 99–104.

[8] D. Mellinger and V. Kumar, "Minimum snap trajectory generation and control for quadrotors," in *2011 IEEE international conference on robotics and automation*. IEEE, 2011, pp. 2520–2525.

[9] M. M. de Almeida, R. Moghe, and M. Akella, "Real-time minimum snap trajectory generation for quadcopters: Algorithm speed-up through machine learning," in *2019 International conference on robotics and automation (ICRA)*. IEEE, 2019, pp. 683–689.

[10] A. V. D. Schaft, "$\mathcal{L}_2$-gain analysis of nonlinear systems and nonlinear state-feedback $\mathcal{H}_\infty$ control," *Transactions on Automatic Control*, vol. 37, no. 6, pp. 770–784, 1992.

[11] A. V. der Schaft, "On a state space approach to nonlinear $\mathcal{H}_\infty$ control," *Systems & Control Letters*, vol. 16, no. 1, pp. 1–8, 1991.

[12] B. A. Francis and J. C. Doyle, "Linear control theory with an $\mathcal{H}_\infty$ optimality criterion," *SIAM J. on Control and Optimization*, vol. 25, no. 4, pp. 815–844, 1987.

[13] G.-W. Van der Linden and P. F. Lambrechts, "$\mathcal{H}_\infty$ control of an experimental inverted pendulum with dry friction," *Control Systems Magazine*, vol. 13, no. 4, pp. 44–50, 1993.

[14] R. A. Nichols, R. T. Reichert, and W. J. Rugh, "Gain scheduling for H-infinity controllers: A flight control example," *Transactions on Control systems technology*, vol. 1, no. 2, pp. 69–79, 1993.

[15] B. E. Sedhom, M. M. El-Saadawi, A. Y. Hatata, and E. E. Abd-Raboh, "A multistage H-infinity-based controller for adjusting voltage and frequency and improving power quality in islanded microgrids," *International Transactions on Electrical Energy Systems*, vol. 30, no. 1, pp. 1–34, 2020.

[16] M. Chilali and P. Gahinet, "$\mathcal{H}_\infty$ design with pole placement constraints: An LMI approach," *Transactions on automatic control*, vol. 41, no. 3, pp. 358–367, 1996.

[17] F. Treves, *Topological Vector Spaces, Distributions and Kernels: Pure and Applied Mathematics*. Elsevier, 2016, vol. 25.

[18] M. Aliyu and E. K. Boukas, "Extending nonlinear $\mathcal{H}_2$, $\mathcal{H}_\infty$ optimisation to $\mathcal{W}_{1,2}$, $\mathcal{W}_{1,\infty}$ spaces - part I: optimal control," *International Journal of Systems Science*, vol. 42, no. 5, pp. 889–906, 2011.

[19] D. N. Cardoso and G. V. Raffo, "Approximated solutions to the nonlinear $\mathcal{H}_2$ and $\mathcal{H}_\infty$ control approaches formulated in the sobolev space," in *European Control Conference*. IEEE, 2018, pp. 1–6.

[20] D. N. Cardoso, S. Esteban, and G. V. Raffo, "Nonlinear $\mathcal{H}_2$ and $\mathcal{H}_\infty$ control formulated in the sobolev space for mechanical systems," in *9th Symposium on Robust Control Design*, 2018, pp. 3812–3817.

[21] D. N. Cardoso, S. R. Esteban, and G. V. Raffo, "A robust optimal control approach in the weighted sobolev space for underactuated mechanical systems," *Automatica*, vol. 125, pp. 1–11, 2021.

[22] D. N. Cardoso, S. Esteban, and G. V. Raffo, "Nonlinear $\mathcal{H}_2$ and $\mathcal{H}_\infty$ control formulated in the weighted sobolev space for underactuated mechanical systems with input coupling," in *IEEE Conference on Decision and Control*, 2018, pp. 3812–3817.

[23] D. E. Kirk, *Optimal control theory: an introduction*. Courier Corporation, 2004.

[24] A. A. Siqueira, M. H. Terra, and B. C. Maciel, "Nonlinear mixed $\mathcal{H}_2/\mathcal{H}_\infty$ control applied to manipulators via actuation redundancy," *Control engineering practice*, vol. 14, no. 4, pp. 327–335, 2006.

[25] B.-S. Chen and Y.-C. Chang, "Nonlinear mixed $\mathcal{H}_2/\mathcal{H}_\infty$ control for robust tracking design of robotic systems," *International Journal of Control*, vol. 67, no. 6, pp. 837–857, 1997.

[26] Y.-C. Chang, "Adaptive $\mathcal{H}_2/\mathcal{H}_\infty$ tracking control for a class of uncertain robotic systems," *International Journal of Control*, vol. 90, no. 3, pp. 463–479, 2017.

[27] G. V. Raffo, M. G. Ortega, and F. R. Rubio, "Nonlinear $\mathcal{H}_\infty$ controller for the quad-rotor helicopter with input coupling," *IFAC Proceedings Volumes*, vol. 44, no. 1, pp. 13 834–13 839, 2011.